Geochronology of impact structures - constraining syn- and post-impact processes using the 40Ar/39Ar and U-Pb techniques

Herrmann, Maria

2020

Document Version:
Publisher's PDF, also known as Version of record

The Meteoritical Society

Meteoritics & Planetary Science 54, Nr 8, 1764–1780 (2019)
doi: 10.1111/maps.13309

An Early Jurassic age for the Puchezh-Katunki impact structure (Russia) based on $^{40}Ar/^{39}Ar$ data and palynology†

S. HOLM-ALWMARK[1,2,3*], C. ALWMARK[1], L. FERRIÈRE[4], S. LINDSTRÖM[5], M. M. M. MEIER[6], A. SCHERSTÉN[1], M. HERRMANN[1], V. L. MASAITIS[7], M. S. MASHCHAK[7], M. V. NAUMOV[7], and F. JOURDAN[8]

[1]Department of Geology, Lund University, Sölvegatan 12, SE-22362 Lund, Sweden
[2]Niels Bohr Institute, University of Copenhagen, Copenhagen, Denmark
[3]Natural History Museum of Denmark, University of Copenhagen, Copenhagen, Denmark
[4]Natural History Museum, Burgring 7, A-1010 Vienna, Austria
[5]Geological Survey of Denmark and Greenland, Øster Voldgade 10, DK-1350 Copenhagen, Denmark
[6]Institute of Geochemistry and Petrology, ETH Zurich, Clausiusstrasse 25, CH-8092 Zurich, Switzerland
[7]Karpinskii All-Russian Geological Research Institute, Srednii pr. 74, St. Petersburg 199026, Russia
[8]Western Australian Argon Isotope Facility, Department of Applied Geology and JdL-CMS, Curtin University, Perth, Western Australia 6845, Australia
[*]Corresponding author. E-mail: sanna.alwmark@geol.lu.se

(Received 26 November 2018; revision accepted 29 April 2019)

Abstract–The Puchezh-Katunki impact structure, 40–80 km in diameter, located ~400 km northeast of Moscow (Russia), has a poorly constrained age between ~164 and 203 Ma (most commonly quoted as 167 ± 3 Ma). Due to its relatively large size, the Puchezh-Katunki structure has been a prime candidate for discussions on the link between hypervelocity impacts and extinction events. Here, we present new $^{40}Ar/^{39}Ar$ data from step-heating analysis of five impact melt rock samples that allow us to significantly improve the age range for the formation of the Puchezh-Katunki impact structure to 192–196 Ma. Our results also show that there is not necessarily a simple relationship between the observed petrographic features of an impact melt rock sample and the obtained $^{40}Ar/^{39}Ar$ age spectra and inverse isochrons. Furthermore, a new palynological investigation of the postimpact crater lake sediments supports an age significantly older than quoted in the literature, i.e., in the interval late Sinemurian to early Pliensbachian, in accordance with the new radioisotopic age estimate presented here. The new age range of the structure is currently the most reliable age estimate of the Puchezh-Katunki impact event.

INTRODUCTION

The inventory of terrestrial impact structures remains largely incomplete due to, for example, the rejuvenation of the crust by erosion, tectonic overprint, and postimpact sedimentary cover. In addition, the ages of a large number of terrestrial impact structures are poorly constrained. In fact, Jourdan et al. (2012) concluded that only 21 of the, at the time, known 179 impact structures on Earth have ages with a precision better than ±2%.

In the present study, we aim at improving the age of the poorly dated ~164 to 203 Ma (Mashchak 1999) Puchezh-Katunki impact structure, located ~400 km northeast of Moscow (Russia). We use new $^{40}Ar/^{39}Ar$ data obtained from impact melt rock samples from the Vorotilovskaya drill core, retrieved from the center of the Puchezh-Katunki impact structure, along with petrographic descriptions of the investigated samples. We also present new biostratigraphic data for the crater lake sediments as well as a reinterpretation of the previously published biostratigraphic data that was the

†This paper is dedicated to the memory of our late colleague and friend Svetlana Bogdanova (1937–2019), without whom this study would not have been possible.

basis for the age determination that resulted in the most commonly quoted age of the Puchezh-Katunki impact event (i.e., 167 ± 3 Ma; Mashchak [1999] and references therein).

GEOLOGICAL SETTING OF THE STRUCTURE AND PREVIOUS AGE ESTIMATES

The Impact Structure

Located in the Privolzhsky Federal District of Russia (N 56°58′, E 43°43′; Fig. 1), ~400 km northeast of Moscow, the Puchezh-Katunki impact structure is buried under Upper Jurassic, Cretaceous, and Cenozoic sediments that together have a maximum thickness of ~100 m (Masaitis and Pevzner 1999). The burial of this impact structure has helped its preservation, but limits its accessibility, as the structure only crops out along the Volga River, on the western edge of the structure. Almost 180 drill holes, one of which reached a depth of 5374 m (i.e., the Vorotilovskaya deep drill hole, VDDH; Fig. 1), have allowed the investigation of the entire structure and its various impactite types (for information on the drilling, see Masaitis and Pevzner 1999).

The impact structure has a complex morphology, with an 8–10 km wide central uplift surrounded by an annular depression. The annular depression is between 1.6 and 1.9 km deep and extends from 8–12 km to 25–30 km radial distance (Figs. 1 and 2) (e.g., Masaitis et al. 1996; Masaitis and Pevzner 1999). At the time of impact, the crystalline basement rocks, dominated by leucocratic and mesocratic gneisses and schists (with minor occurrences of amphibolite, mafic, and ultramafic rocks), were overlain by Upper Proterozoic to Lower Mesozoic sedimentary rocks. This sequence of sedimentary rocks is well known from nearby areas surrounding the impact structure. The 1.8–2.2 km thick sequence is composed of 500 m of Neoproterozoic clastics, 800 m of Devonian limestone and shale; 450 m of Carboniferous carbonates and marl; 250 m of Lower Permian carbonates, evaporites, and clay; 160 m of Upper Permian clastics; and 80 m of Lower Triassic clay and siltstone (Masaitis et al. 1996; Masaitis and Pevzner 1999). After the impact crater formed, it was filled by a lake in which up to 450 m of clay and clastic sediments were deposited (including a unit of gritstone and sandstone made up by reworked impactites, and the overlying so-called Kovernino Formation; Masaitis et al. [1996] and references therein).

The rim-to-rim diameter of the collapsed transient crater of the Puchezh-Katunki impact structure is 40 km (e.g., Earth Impact Database 2019), whereas the ~80 km diameter mentioned in previous studies (e.g., Feld'man et al. 1984; Masaitis et al. 1996; Masaitis 1999; Pálfy 2004) rather represents a maximum "damage diameter" estimate.

Impactites

The central uplift of the Puchezh-Katunki impact structure (Fig. 2) is composed mainly of authigenic breccia of shocked Precambrian gneisses and amphibolites, with minor occurrences of Neoproterozoic argillites and Devonian carbonates. The uplift has a central pit, up to 500 m deep, and is partly overlain by thin layers of polymict lithic breccias, melt-bearing breccias (traditionally referred to as "suevite"; see recent discussions on this term in Grieve et al. 2015; Stöffler 2015), reworked impactites, and crater lake sediments of the Kovernino Formation (Masaitis et al. 1996). The thickness of the crater lake deposits in the central pit is 306 m. The annular depression surrounding the central uplift is filled with an allochthonous megabreccia composed of blocks of sedimentary rocks, polymict lithic breccias (i.e., both coarse- and fine-grained varieties which are dominated by sedimentary clasts), and melt-bearing breccias, and in turn is overlain by the Kovernino Formation. Outside of the annular depression, disturbed Permian and Triassic sedimentary rocks are covered by a polymict lithic breccia with sedimentary clasts that is ~100 m thick (Masaitis and Pevzner 1999).

The crater fill lithologies from Puchezh-Katunki (Figs. 1 and 2) are dominated by diverse allochthonous lithic breccias that are distributed in the annular depression, overlie parts of the central uplift, and cover the area outside of the annular depression, out to a radial distance of ~35 km (maximum 41.5 km; Masaitis and Pevzner 1999). Impactites are found on the slopes of the central uplift as irregular bodies and lenses up to 116 m thick, including melt-bearing breccias and impact melt rocks (traditionally referred to as "tagamite").

Impact melt rocks occur either as injected veins (with maximum thickness of 3 m) within the crystalline rocks of the central uplift, or as irregular bodies, up to 10 m in thickness, within allochthonous polymict lithic breccia on the southwestern slope of the central uplift. The impact melt rocks from the allochthonous breccia have marginal parts that are vesicular, typically with abundant clasts (up to 35–40% of the total rock) of claystone, sandstone, and gneiss with clast sizes from less than a millimeter up to a few centimeters (maximum size 10–15 cm; Masaitis and Pevzner 1999). In the central parts of these impact melt rock occurrences, clasts are usually much less abundant (representing a maximum of 15% of the total rock), and the matrix is aphanitic and nonvesicular (Masaitis and Pevzner 1999). The impact melt rocks of the central uplift are variable in texture and are best studied in the core samples recovered from the VDDH, with the following varieties identified from previous studies: holohyaline, cryptocrystalline, hyalopilitic, and hemicrystalline (Masaitis and Pevzner 1999). At the

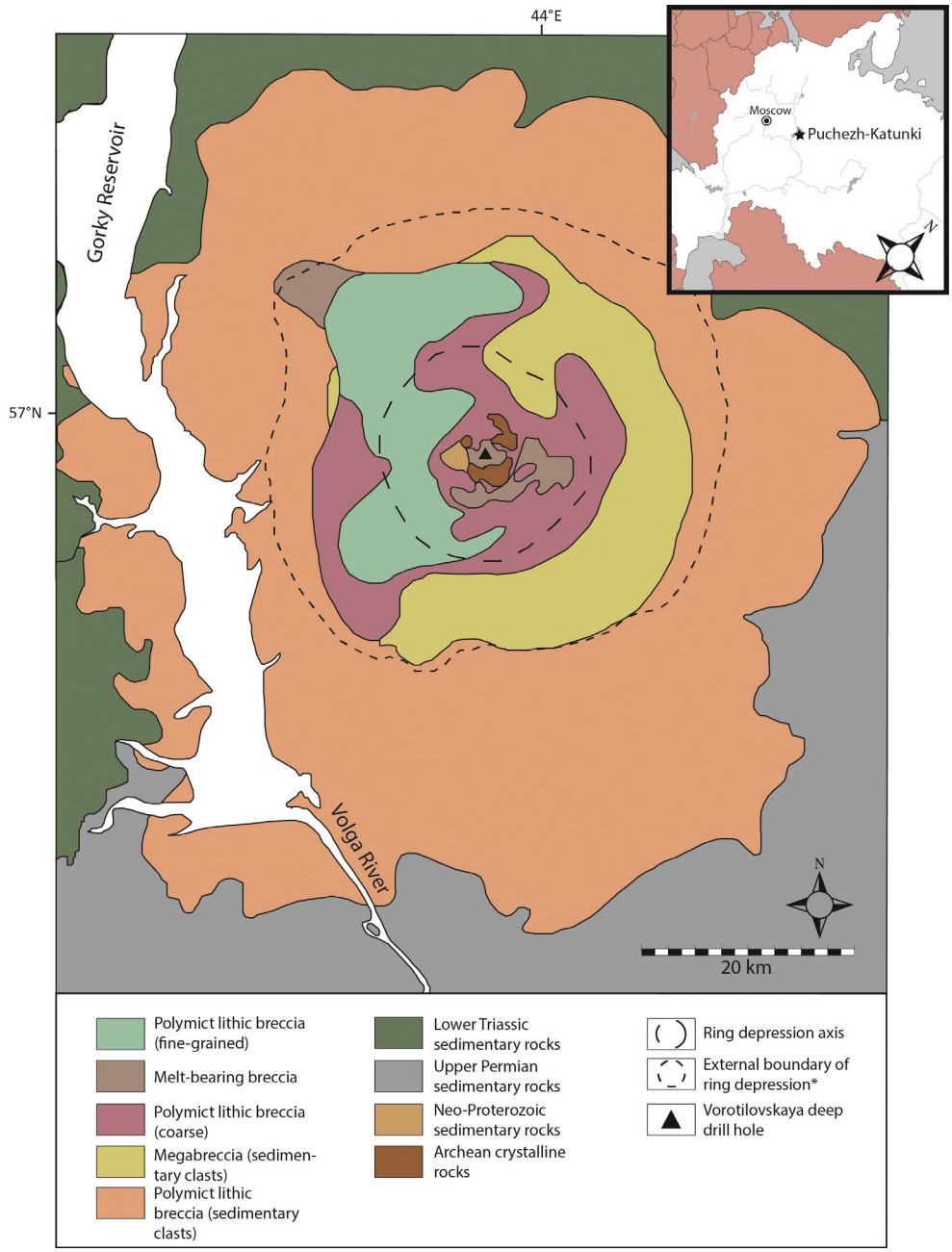

Fig. 1. Geological map of the Puchezh-Katunki impact structure (after Masaitis et al. 1996). The inset map shows the location of the impact crater in Russia. The crater lake and younger deposits are not displayed on the map. *Coinciding with the distribution area of the crater lake sediments. (Color figure can be viewed at wileyonlinelibrary.com.)

macroscopic scale, they are usually dark gray or black in color, massive or vesicular, and display sharp contacts with the host rocks (Masaitis and Pevzner 1999).

Previous Age Determinations

The first reported Late Triassic to Early Jurassic age for the Puchezh-Katunki impact was based on stratigraphy (Firsov 1973). The most commonly quoted age of 167 ± 3 Ma (i.e., Bajocian, Middle Jurassic; Cohen et al. 2013, updated) was based on palynostratigraphic analysis performed by G. E. Donskova on the oldest crater lake sediments, and reported in Bogorodskaya and Tumanov (1980), Masaitis et al. (1996), Masaitis (1999), and Masaitis and Pevzner (1999). Feld'man et al. (1984) concluded that the lacustrine section of the crater fill sediments

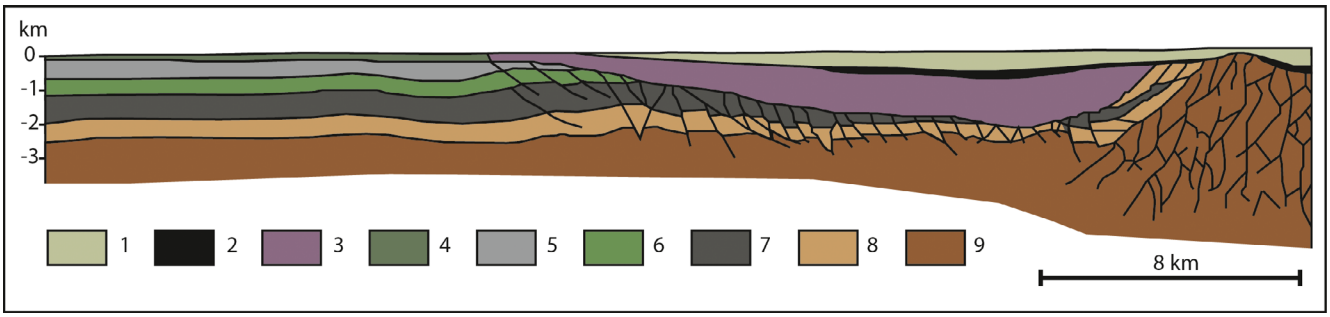

Fig. 2. Geological cross section of the northwestern sector of the Puchezh-Katunki impact structure (after Masaitis et al. 1996). Note that sediments younger than the crater lake deposits are not displayed in this figure. (1) Crater lake deposits (Kovernino Formation); (2) polymict fine-grained breccia, melt-bearing breccia ("suevite"; see text), and polymict lithic breccia (coarse); (3) sedimentary megabreccia (right side of the section) and sedimentary polymict lithic breccia (coarse; left side of the section); (4) Triassic sediments; (5) Permian sediments; (6) Carboniferous sediments; (7) Devonian sediments; (8) Neoproterozoic sediments; and (9) Archean crystalline rocks. (Color figure can be viewed at wileyonlinelibrary.com.)

does not relate to the time of the impact, and instead suggested a considerably older age of ~215–220 Ma, which was constrained by impact ejecta (glass fragments) in Triassic sediments. In addition, Pálfy (2004) discussed the commonly quoted 167 ± 3 Ma biostratigraphic age and concluded that it was problematic, as the presented data were not sufficient (i.e., only a taxonomic list and their abundances, no photographs, were presented), and that the methods practiced in the older publications used a taxonomic terminology and methodology that differed from those used by Western palynologists. Schmieder and Buchner (2008) explored the age of the Puchezh-Katunki impact by applying a paleogeographical method. They concluded, based on the presence of lacustrine sediments in the Puchezh-Katunki crater infill, that the structure has a minimum age in the range of Late Triassic to early Middle Jurassic (>170 Ma), when most parts of the Russian Platform were continental. According to these authors, after Bajocian or Bathonian time, marine sediments were deposited in the area.

Radioisotopic dating techniques have also been applied to samples from the Puchezh-Katunki impact structure. Mashchak (1999) reported five K/Ar ages that range from 183 ± 5 Ma to 200 ± 3 Ma. However, K/Ar ages have been shown to be unsuitable to confidently date impact events, as it is not possible to characterize the effect of alteration and the loss of $^{40}Ar^{*}$ (causing younger apparent ages) and/or extraneous (excess and/or inherited) ^{40}Ar (causing older apparent ages; see Jourdan 2012; Jourdan et al. 2012). Mashchak himself considered the ages he obtained to result from contamination of the investigated impact melt samples by old Archean target lithologies, and thus favored the younger palynological age for the impact event.

MATERIAL AND METHODS

Samples

Samples for Ar-Ar Dating

Veins of impact melt rock from five different levels of the upper parts of the 5374 m deep VDDH were sampled for this study: V931, V1018, V1144, V1218, and V1251 (note that the sample names correspond to depth below the surface in meters; Fig. 3). The veins are curved and branched, 1–10 cm thick, and can be massive or vesicular in texture. The vesicular varieties are typically more altered than the massive samples, with more prominent chlorite and/or clay mineralization. Chemical analyses of similar impact melt rock samples were presented by Masaitis and Pevzner (1999), showing that although the chemical composition can vary from one sample to another, all of them show a composition close to the average composition of all impact melt rocks from Puchezh-Katunki. This average composition corresponds to a mixture of amphibolite–biotite gneisses and amphibolites in a ratio of 4:1.

The samples selected for this study all differ from one another in terms of texture, content of clasts, and abundance of vesicles (Fig. 4). They range from holocrystalline (samples V1144, V1218, and V1251) to hypohyaline (samples V931 and V1018), and they all contain clasts of various sizes. Based on their different characteristics, we have grouped our samples into three different varieties: type A (sample V931), type B (sample V1018), and type C (samples V1144, V1218, and V1251).

Sample V931, Type A

Sample V931 (Fig. 4a) is a gray, compact impact melt rock. Petrographic investigations reveal a dark brown to black, partly glassy, microcrystalline matrix

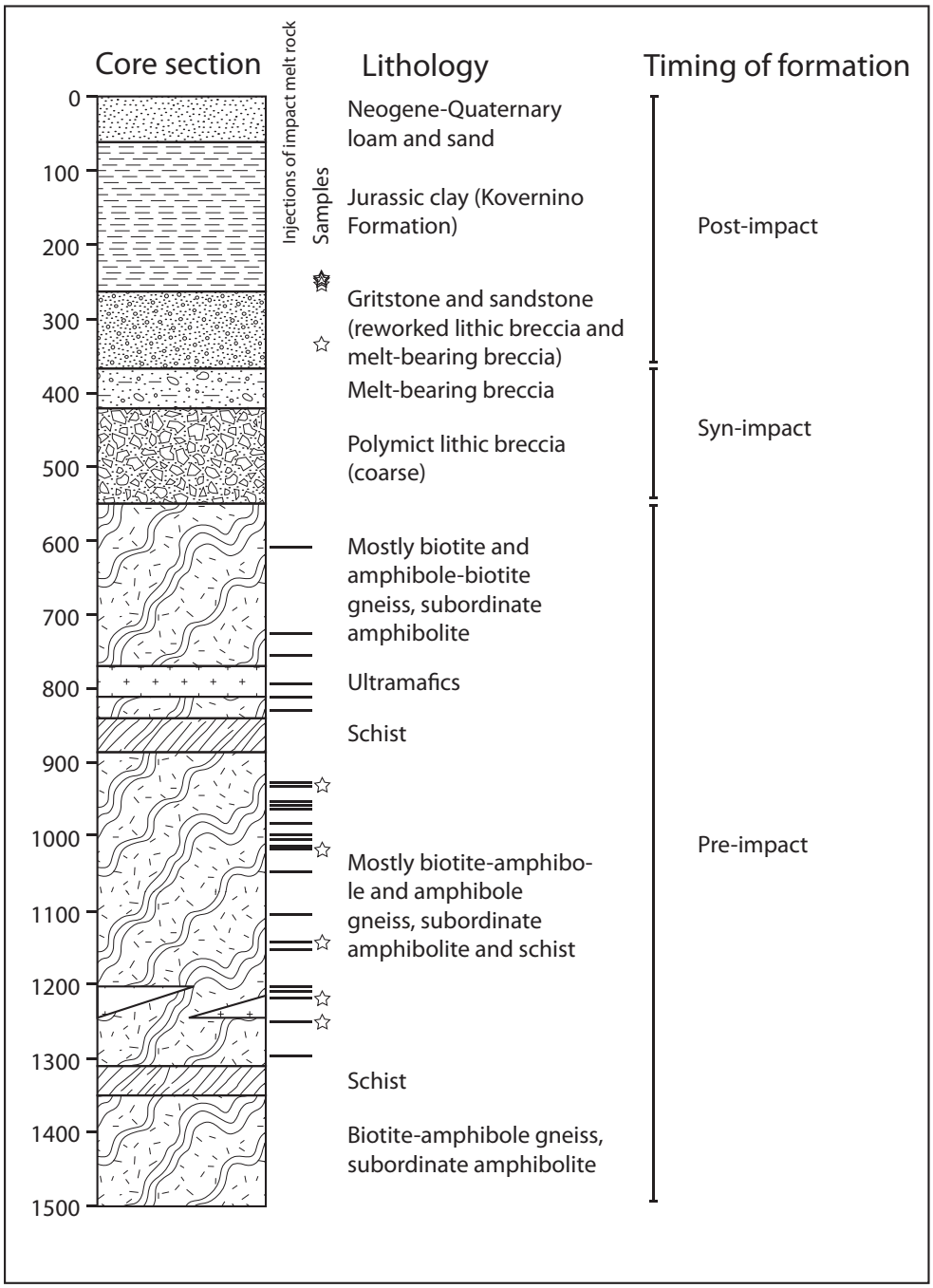

Fig. 3. Lithological description of the upper part of the Vorotilovskaya deep drill core. Stars mark the intervals that were sampled in this study.

with flow texture (Figs. 5a and 5b). The glass is partly devitrified and/or hydrothermally altered to phyllosilicate minerals, resulting in a greenish-brown color, with the occurrence of opaque phases. The sample is composed of two different phases, one darker, more glassy, and less devitrified, with lower clast content than in the other one, whereas the other phase is more devitrified and contains up to ~40% clasts. The investigated thin sections contain schlieren of polycrystalline ("mosaic") quartz (Fig. 5b). The nature of the clasts is the same in the two phases; they consist of lithic rock clasts dominated by quartz and feldspar, and single crystals of quartz, feldspar, and opaque minerals. The contact between clasts and

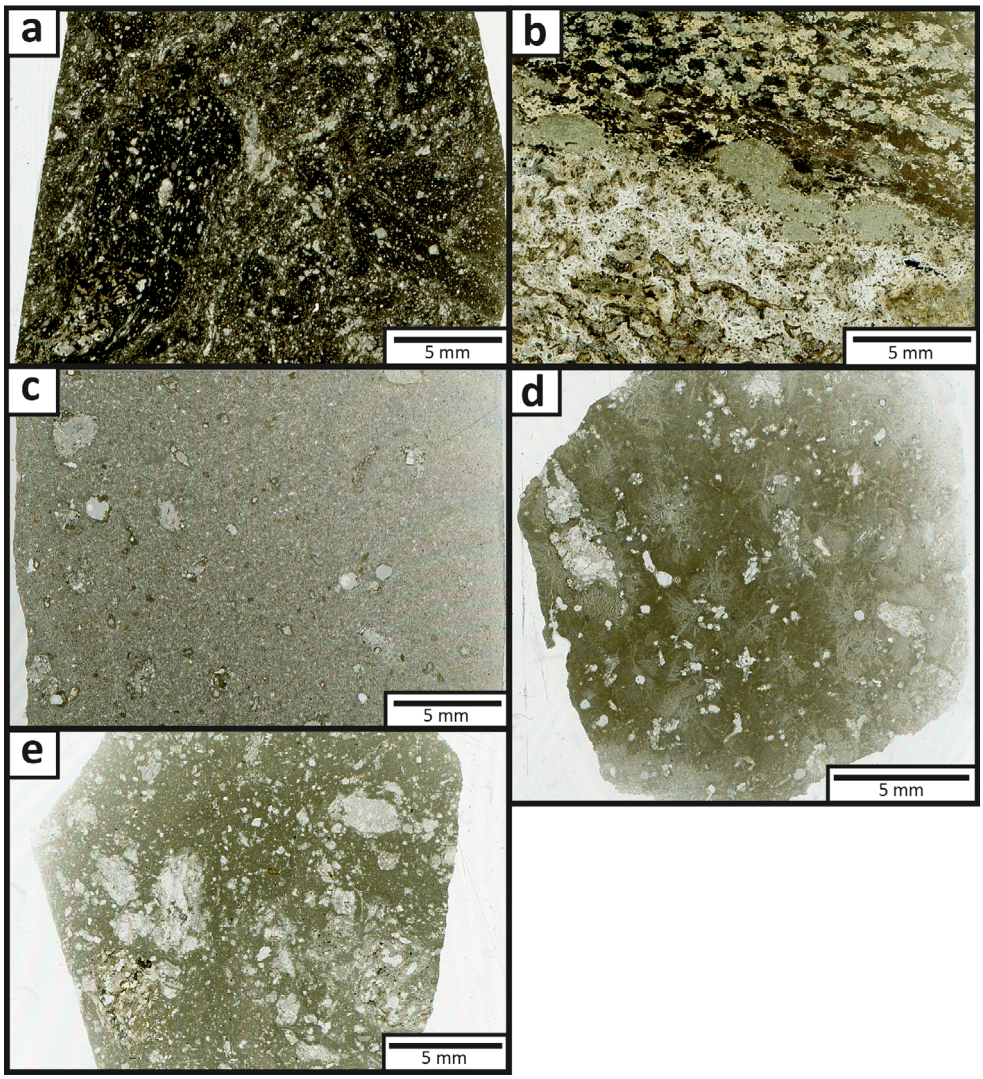

Fig. 4. Scanned polished thin sections of the investigated impact melt rock samples from Puchezh-Katunki. a) Sample V931 (Type A). b) Sample V1018 (Type B). c) Sample V1144 (Type C). d) Sample V1218 (Type C). e) Sample V1251 (Type C). (Color figure can be viewed at wileyonlinelibrary.com.)

matrix is irregular (with subrounded clasts), indicating partial assimilation of the clasts by the melt (Fig. 5a). Around some of the single quartz clasts, a corona of tiny pyroxene crystals is visible (Fig. 6c). The quartz clasts and quartz grains in the lithic rock fragments are partly or entirely finely crystalline, showing a "mosaic texture." The rest of the quartz grains are toasted and/or show one or more sets of shock-induced planar microstructures (Fig. 5a). Some of the grains display a microtexture that is very similar to ballen silica, but their precise nature could not be fully resolved. Alteration of feldspar makes it difficult to identify the presence of shock-induced features; however, some grains display optically isotropic areas that appear to be diaplectic glass.

Sample V1018, Type B

Sample V1018 (Fig. 4b) is a gray, compact, melt rock with flow texture. Petrographic investigations reveal a "banded texture," with three different "regions." The sample is clast-poor, with the only clasts being ilmenite and apatite grains. These clasts show no signs of melting or reaction with the matrix. The three distinct "regions" are composed of (1) a light-colored material with fibrous crystals of zeolite, with some inclusions of recrystallized quartz, which are surrounded by aphanitic, dark and glassy, material (Fig. 5c); (2) a greenish area dominated by saponite crystals (~10 μm in size); and (3) a brown area that is microcrystalline with abundant Fe-rich and Ti-rich opaque grains and aggregates of saponite, with pockets of needle-like recrystallized plagioclase.

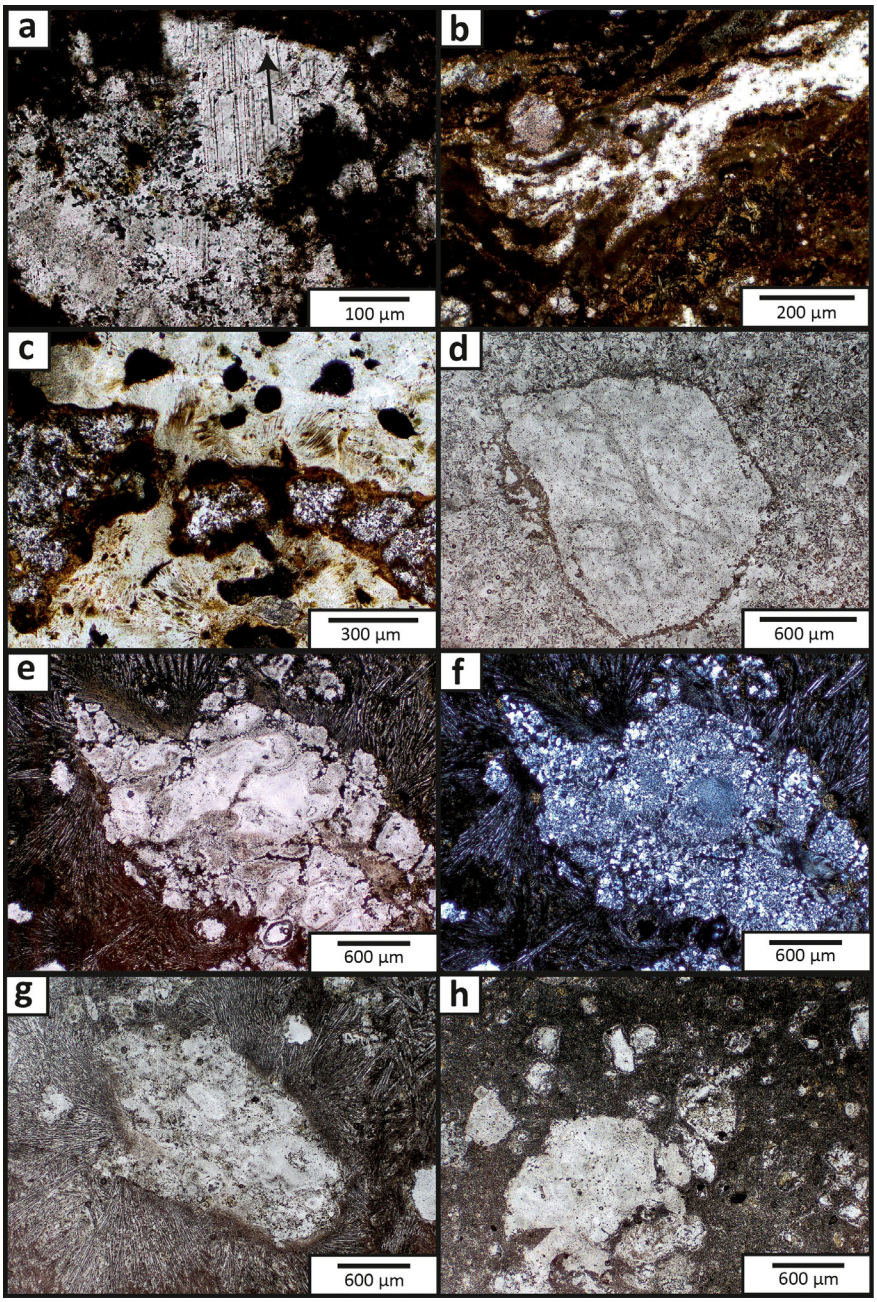

Fig. 5. Thin section photomicrographs of Puchezh-Katunki impact melt rocks. a) Sample V931 (plane-polarized light; PPL). Lithic clast dominated by quartz showing one set of shock-induced planar microstructures (marked by an arrow). The grain also shows a melt-clast boundary reaction, with part of the grain being assimilated. b) Sample V931 (PPL). Schlieren of finely crystalline mosaic quartz in a devitrified matrix with flow texture. c) Sample V1018 (PPL). Light-colored region, dominated by zeolite with opaque phases (rounded black areas) and pockets of finely crystalline mosaic quartz (white areas), surrounded by melt (black regions on boundaries) that is partly devitrified (brown). d) Sample V1144 (PPL). Large clast of polycrystalline quartz in a matrix dominated by plagioclase needles and pyroxene crystals. Note the clast-matrix boundary where a finely crystalline accumulation of minerals, also found in vesicles, can be observed. e) Sample V1218 (PPL). Large clast dominated by polycrystalline silica after lechatelierite. Note the texture of the matrix with plagioclase needles radiating outwards from the clast. f) Same view as in (e), in crossed polarizers. g) Sample V1218 (PPL). Large clast dominated by polycrystalline silica forming "blobs." Note the needles of plagioclase radiating outwards from the clast, forming aggregates. h) Sample V1251 (PPL). Overview of the fine-grained crystalline matrix and abundant inclusions of polycrystalline quartz with rounded boundaries to the surrounding matrix. Note the clasts in the upper part of the photograph with a black rim of pyroxene surrounded by a clear area of recrystallized silica. (Color figure can be viewed at wileyonlinelibrary.com.)

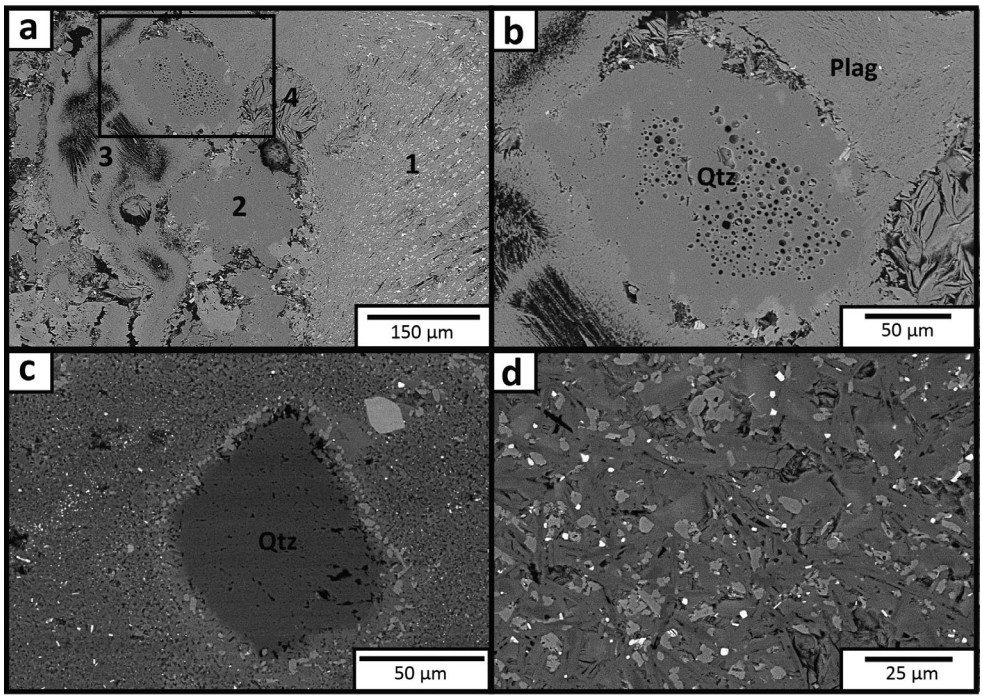

Fig. 6. Backscattered electron images of Puchezh-Katunki impact melt rock. a) Sample V1218. (1) Matrix with needle-shaped crystals of plagioclase, minute crystals of pyroxene, and opaque minerals; (2) clast consisting of polycrystalline quartz; (3) fibrous zeolite; and (4) saponite-filled vesicle. Box indicates area that is enlarged in (b). b) Close-up of part of the (a) photomicrograph showing vesicles in quartz. c) Clast of quartz in sample V931 showing crystals of pyroxene lined up along the grain-matrix boundary. d) Close-up of fine-grained crystalline matrix in sample V1251. Dark gray = plagioclase needles, lighter gray = pyroxene, and white = opaque minerals.

Sample V1144, Type C

Sample V1144 (Fig. 4c) is a gray, vesicular impact melt rock with elongated vesicles, 1–5 mm in size, and some clasts. Petrographic investigations show that it is a well-crystallized, clast-poor impact melt rock. The matrix is fine-grained and consists mainly of needle-shaped plagioclase (up to 100 μm in size), pyroxene, quartz, opaque minerals, and an extremely fine-grained "clayey" phase (the nature of which is undetermined). Clasts are isolated and consist either of polycrystalline and dusty/cloudy quartz (Fig. 5d) or a mixture of partly polycrystalline quartz, calcite, and mafic minerals. Pockets of fibrous aggregates of secondary zeolite also occur. The silica-rich inclusions are often surrounded by a brown-greenish, fine-grained material (Fig. 5d) that also partly or completely fills vesicles together with quartz. The clasts have irregular contacts with the matrix that in places have started to assimilate.

Sample V1218, Type C

Sample V1218 (Fig. 4d) is a gray melt rock with small, 1–2 mm in size, spherical vesicles. Petrographic investigations show a crystalline matrix dominated by needle-shaped plagioclase (up to ~1 mm long). Plagioclase forms quench-textured star-shaped aggregates together with pyroxene and minute titanite crystals in a brown fine-grained material. Finely crystalline mosaic quartz dominates the clasts (Figs. 5e and 5f). Pockets of fibrous aggregates of zeolite also occur. The quartz clasts are dusty in appearance, owing to the presence of tiny vesicles, 1–2.5 μm in size (Figs. 6a and 6b), and are often rimmed with minute crystals of pyroxene and opaque minerals. The contact between the clasts and the matrix is irregular, and some clasts show preserved melt texture (Fig. 5e). Some quartz-dominated clasts show a spherical texture (Fig. 5g), most likely explained by devitrification of microperlitic texture, implying that the clasts were once molten. The vesicles are partly, and in some cases completely, filled by saponite, with rare occurrences of chlorite and zeolite, together with quartz.

Sample V1251, Type C

Sample V1251 (Fig. 4e) is a gray, compact melt rock with clasts. The investigated sample contains a centimeter-sized gneiss clast. Petrographic investigations reveal a very fine-grained crystalline matrix (Figs. 5h and 6d) with needle-shaped plagioclase; minute pyroxene crystals; ilmenite; and altered, dark brown, fine-grained material. Clasts are more or less rounded and dominated by polycrystalline quartz, which in some

cases are rimmed by minute crystals of pyroxene and, in turn, are surrounded by a corona of clear silica glass (Fig. 5h). Some of the quartz clasts show preserved diaplectic glass in their center. Recrystallized ballen silica, now quartz (type V; Ferrière et al. 2009) is present. Some of the quartz clasts are derived from partly digested and broken-up lithic clasts, in which titanite and apatite crystals are also observed.

Samples for Palynological Analysis

Six samples from the upper part of the VDDH were prepared for palynological analysis; V245.20, V245.40, V249.20, V251.60, V256.80, and V337.00 (with sample names corresponding to the depth at which they were taken; Fig. 3). The upper five samples are from the Kovernino Formation, whereas the lowermost sample (i.e., V337.00) was taken in an interval of the core that is composed of gritstone and sandstone (i.e., made up of reworked impactites).

METHODOLOGY

Two thin sections were prepared from each of the five impact melt rock samples. These were studied using a standard petrographic microscope, and further investigations and phase determinations were performed using an energy dispersive X-ray spectrometer (Inca X-sight, Oxford instruments), linked to a Hitachi S-3400N scanning electron microscope at Lund University.

$^{40}Ar/^{39}Ar$ Dating

Each of the five samples were crushed by hand in an agate mortar and cleaned in deionized water and ethanol. The samples were then sieved, and clean fragments (i.e., showing minimum signs of alteration and not containing visible clasts) were hand-picked from the 250–500 μm fraction under an optical microscope resulting in five ~20 mg samples.

The hand-picked samples were irradiated together with the Taylor Creek sanidine standard (initially assumed to be 28.34 Ma, recalculated by Renne et al. 1998, and later revised to 28.608 ± 0.033 Ma; Renne et al. 2011) for 18 h at the Oregon State University research reactor, USA. *J*-values were calculated with a precision better than 0.25% (2σ) and the uncertainties in the *J*-values were propagated into the uncertainties included in the plateau ages. At the time of analysis, in 2015, the data were all reduced using the decay constants from Steiger and Jäger (1977). Due to recent revision of the decay constant and for comparison with the stratigraphic time scale (Cohen et al. 2013, updated) and to other impact ages listed by Jourdan et al. (2012), $^{40}Ar/^{39}Ar$ ages presented in this study have been recalculated using the revised ^{40}K decay constants and monitor ages of Renne et al. (2011). Analytical and *J*-value uncertainty are provided with each $^{40}Ar/^{39}Ar$ apparent age and the final age recommended for the impact event is given together with all sources of uncertainty.

The samples were analyzed in the $^{40}Ar/^{39}Ar$ geochronology laboratory at Lund University, Sweden. The laboratory has a Micromass 5400 mass spectrometer with a Faraday cup and an electron multiplier. The mass spectrometer is connected to a metal extraction line, which contains two SAES C50-ST101 Zr-Al getters and a cryogenic cold finger cooled to approximately −155°C by a Polycold P100 cryogenic refrigeration unit. All sample aliquots were loaded into a copper planchette containing multiple 3 mm diameter holes. Samples were step-heated using a defocused 50 W CO_2 laser. Sample clean up time was 5 minutes. The laser was rastered over the samples to provide even heating of the sample. The entire analytical process is fully automated through MassSpec, a software modified specifically for this laboratory and originally developed by Al Deino at the Berkeley Geochronology Center, USA. Time zero regressions were fitted to data collected from 10 scans over the 40–36 mass range. Peak heights and backgrounds were corrected for mass discrimination, isotopic decay, and interfering nucleogenic reactor Ca-, K-, and Cl-derived isotopes. Isotopic production values for the cadmium-lined position in the OSU reactor are $^{36}Ar/^{37}Ar(Ca) = 0.000264$, $^{39}Ar/^{37}Ar(Ca) = 0.000695$, and $^{40}Ar/^{39}Ar(K) = 0.00073$. Argon-40 blanks were calculated before every new sample and after every three sample steps. Blank values were subtracted for all incremental steps from the sample signal. We were able to produce very good incremental gas splits using a combination of increasing time at the same laser output followed by increasing laser output. Age plateaus were determined using the criteria of Jourdan (2012), which specify that to be considered reliable, a plateau must contain at least 70% of the total ^{39}Ar released. In this paper, we also use the term "mini-plateau," as defined by Jourdan (2012) as a flat section containing between 50% and 70% of the total ^{39}Ar released. The $^{40}Ar/^{39}Ar$ plateau ages are quoted with uncertainties of 2σ (standard error), and the complete data tables for all the sample splits are shown in Appendix S1 in supporting information.

Re-Evaluation of Previously Published Palynology

The taxonomic approach used on the previously published palynological assemblages that formed the basis for the commonly quoted 167 ± 3 Ma age of the Puchezh-Katunki impact (Bogorodskaya and Tumanov 1980; Mashchak 1999) consisted of a combination of

form taxa, fossil, and extant plant taxa, primarily based on the studies of Bolkhovitina (1956, 1959). This approach is in many respects fundamentally different from the standard form taxonomy normally used for Jurassic spores and pollen in Europe (e.g., Batten and Koppelhus 1996). For this reason, we carefully re-evaluated the photographs and sketches of the specific taxa in the original publications by Bolkhovitina (1956, 1959), and the ones published in subsequent papers by other authors (e.g., Jaroshenko 1965; Ilyina 1985, 1986; Goryacheva 2011).

Lower Jurassic to lower Middle Jurassic strata are generally missing on the Russian platform, with shallow marine, coastal, and terrestrial strata of Bajocian and Bathonian age commonly comprising the oldest Jurassic rocks in the region (Mitta et al. 2012). Therefore, the present re-evaluation of the palynology of the Puchezh-Katunki impact structure is based on an interpolation of stratigraphic ranges of selected spore-pollen taxa from independently dated (ammonites and dinoflagellate cysts) palynozonations in western Siberia (Ilyina 1985; Goryacheva 2011) and northwestern Europe (Batten and Koppelhus 1996), as well as spore-pollen floras from Caucasus (Jaroshenko 1965). A few Middle Jurassic assemblages from the Russian Platform (Dobrutskaja 1968; Rostovtseva 2013, 2014) have also been taken into account. According to Rostovtseva (2013), Middle Jurassic palynological assemblages of the Moscow region are very similar to palynofloras reported by Nielsen et al. (2010) from Bornholm (Denmark), thus a comparison with the northwestern European palynozonation may be warranted. The palynological age assessment reported herein uses cumulative maximum and minimum ages for the assemblages, coupled with additional restrictions based on abundance data for some taxa, and/or the lack of taxa otherwise indicative of a certain age according to the literature.

Palynological Preparation and Analysis

The samples were processed using standard palynological methods at the Palynological Laboratory, Geological Survey of Denmark and Greenland (GEUS). Approximately 20 g of sediment from each sample was washed and cleansed, dried, and subsequently crushed in a mortar. The crushed sample was digested in hydrochloric and hydrofluoric acids to dissolve carbonate and silicate minerals, respectively. Heavy liquid separation was used to remove heavy minerals from the organic residues. The organic residues were then mildly oxidized with Schultze's reagent (an aqueous solution of $KClO_3$ and HNO_3) and sieved on a 11 μm mesh filter. Strew slides were curated with glycerin gel and examined under a light microscope.

RESULTS

$^{40}Ar/^{39}Ar$ Dating

Laser step-heating experiments of five whole-rock samples of impact melt rock from the Puchezh-Katunki impact structure were run in duplicate. The obtained $^{40}Ar/^{39}Ar$ age spectra, K/Ca ratios, and inverse isochrons are shown in Figs. 7 and 8, and a summary of the $^{40}Ar/^{39}Ar$ results is provided in Table 1 (for the complete data sets for all the sample splits, see Appendix S1).

The data from partly glassy and microcrystalline sample V931 did not yield any plateau or statistically significant inverse isochron from either of the two analyzed splits. Run V931A yielded a disturbed age spectrum with apparent step ages ranging from ~186 to 336 Ma. The spectrum from V931B is slightly hump-shaped with younger apparent step ages (~167 to 177 Ma) in the low- and high-temperature steps, and older ages of ~197 Ma in the mid-temperature steps.

The two runs of partly glassy sample V1018 yielded one mini-plateau with a date of 196.3 ± 0.82 Ma (mean square weighted deviation [MSWD] = 0.18, probability [P] = 0.97, containing 58% of the released ^{39}Ar). The low-temperature steps of run V1018A reveal one significantly younger apparent age of 106 Ma, and the high-temperature steps move toward older apparent ages (~202–215 Ma). Sample V1018A yielded a mini-inverse isochron age of 193.2 ± 2.0 Ma (MSWD = 0.41; P = 0.80, initial $^{40}Ar/^{36}Ar$ = 299 ± 6, n = 6). In contrast, run V1018B did not produce any plateau or inverse isochron.

Age spectra from both runs (A and B) of the well-crystallized sample V1144 are U-shaped, indicating the presence of inherited or excess ^{40}Ar (see Bottomley et al. 1990; McDougall and Harrison 1999; Kelley 2002), and the three youngest steps in each split yielded apparent ages around 190 Ma, respectively. The data from this sample did not yield statistically significant isochrons. However, the features of the inverse isochron plots for this sample do indicate the presence of two distinct reservoirs of trapped ^{40}Ar (Schmieder et al. 2010, 2015), as the data points follow two correlation lines (not shown, Appendix S1).

Of the two analyzed splits of the well-crystallized sample V1218, V1218A yielded a plateau age of 193.7 ± 1.1 Ma that includes ~79% of the total ^{39}Ar released over five steps (MSWD = 0.41; P = 0.75). The data did not define a statistically valid inverse isochron. The steady increase of individual step ages in the last 15% of the age spectrum is commensurate with a sharp increase in the Ca/K ratio for this sample (Fig. 7), suggesting the presence of undegassed high-Ca clasts. Run V1218B yielded a slightly U-shaped spectrum and

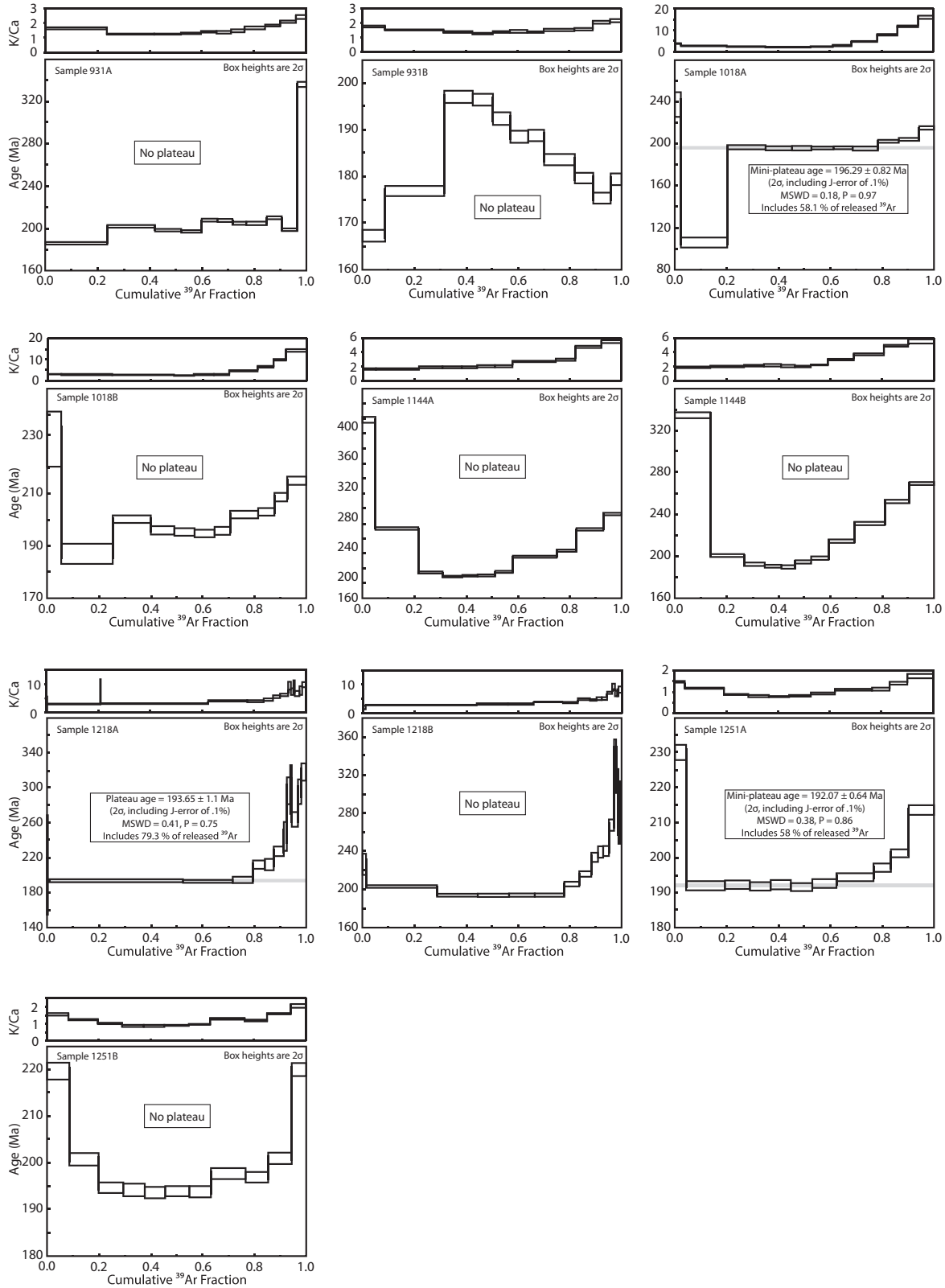

Fig. 7. $^{40}Ar/^{39}Ar$ age spectra and Ca/K ratios for five whole-rock aliquots of impact melt rock from the Puchezh-Katunki impact structure. Each sample was run as two subsamples (A corresponds to run 1 and B to run 2). 2σ errors are shown in the age spectra.

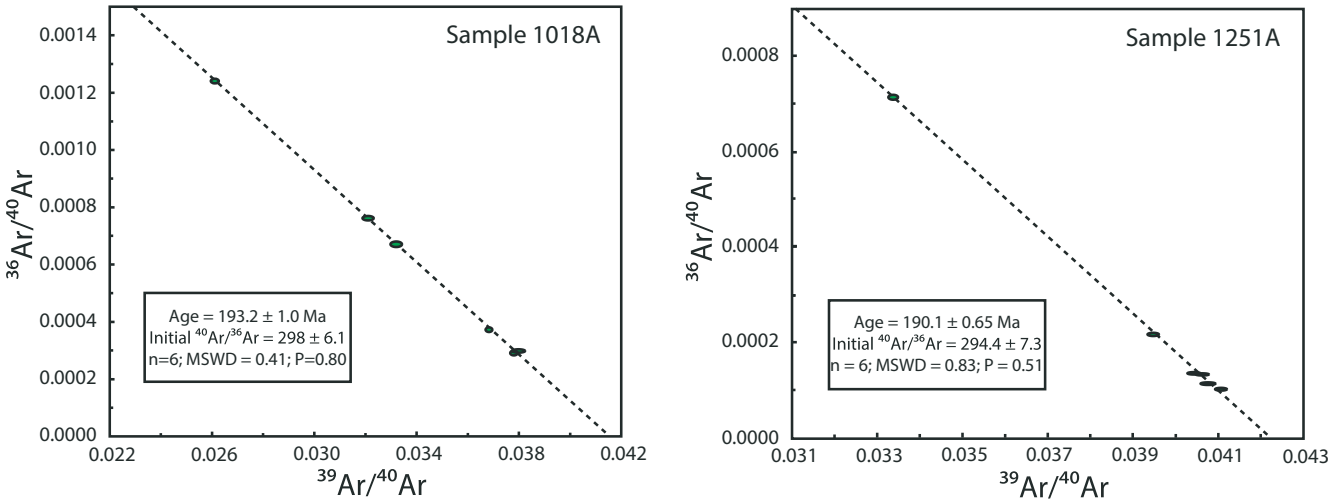

Fig. 8. Inverse isochron plots for samples of Puchezh-Katunki impact melt rock. Errors on ages are given at the 1σ level. (Color figure can be viewed at wileyonlinelibrary.com.)

Table 1. Summary of plateau, mini-plateau, and inverse isochron data from the Puchezh-Katunki impact melt rock samples.

Sample (run)	Apparent age (Ma ± 2σ)	Spectrum characteristics	Total ^{39}Ar released over (mini-) plateau (%)	*n* (steps)	MSWD	*P*	Inverse isochron age (Ma ± 2σ)	MSWD	*P*	$^{36}Ar/^{40}Ar$ intercept
V931(A)	–	No plateau	–	–	–	–	–	–	–	–
V931(B)	–	No plateau	–	–	–	–	–	–	–	–
V1018(A)	196.3 ± 0.8	Mini-plateau	58.1	6	0.18	0.97	193.2 ± 2.0	0.41	0.80	298 ± 6
V1018(B)	–	No plateau	–	–	–	–	–	–	–	–
V1144(A)	–	No plateau	–	–	–	–	–	–	–	–
V1144(B)	–	No plateau	–	–	–	–	–	–	–	–
V1218(A)	193.7 ± 1.1	Plateau	79.3	5	0.41	0.75	–	–	–	–
V1218(B)	–	No plateau	–	–	–	–	–	–	–	–
V1251(A)	192.1 ± 0.6	Mini-plateau	58.0	6	0.38	0.86	190.1 ± 1.3	0.83	0.51	294 ± 7
V1251(B)	–	No plateau	–	–	–	–	–	–	–	–
			Age span:	192–196 Ma						

failed to form a mini-plateau; however, the spectrum contains a section of four consecutive mid-temperature step ages around ~194 Ma that include ~49% ^{39}Ar.

Analysis of two splits of the well-crystallized sample V1251 show that V1251A yielded a mini-plateau that constitutes 58% of the released ^{39}Ar, with a date of 192.07 ± 0.64 Ma (MSWD = 0.38, $P = 0.86$, $n = 6$) and a corresponding mini-inverse isochron age of 190.1 ± 1.3 Ma (MSWD = 0.8, $P = 0.51$, initial $^{40}Ar/^{36}Ar$ = 294 ± 7, $n = 6$). Split V1251B failed to give a plateau age, again indicating the presence of inherited or excess ^{40}Ar.

Biostratigraphy

Results of the Re-Evaluation of Published Palynology

Our re-evaluation resulted in new palynological age estimates for the four spore-pollen assemblages reported from different parts of the Puchezh-Katunki impact structure by Masaitis and Pevzner (1999), and these are briefly summarized below. For the full results, see Appendix S2 in supporting information and for details on the core samples, see Masaitis and Pevzner (1999).

The listed assemblages from the brecciated Neoproterozoic to Lower Triassic rocks on the northeastern slope of the central uplift, as well as from the allogenic breccias in core 17 (located in the northeastern part of the central depression) suggest a maximum–minimum age of early Pliensbachian–early Aalenian (approximately 191–170 Ma), but are most likely restricted to the Pliensbachian (approximately 191–183 Ma). This is based primarily on the obtained composite range for *Paleoconiferus asaccatus*, which has a common occurrence in Hettangian to early Pliensbachian strata, with only rare occurrences in late

Pliensbachian to early Aalenian strata, and is absent from younger Jurassic assemblages (Goryacheva 2011; Ilyina 1985, 1986; Jaroshenko 1965). The restriction to the Pliensbachian is based on the co-occurrence of *P. asaccatus* and *Lycopodiumsporites subrotundus*, with the latter seemingly having its first occurrence in the Pliensbachian (Goryacheva 2011; Ilyina 1985). The assemblage from core 17 also contains *Lycopodiumsporites marginatus* (first occurrence late Pliensbachian; Goryacheva 2011), which indicates a late Pliensbachian maximum and early Aalenian minimum age. However, one of the problems with Early Jurassic palynostratigraphy of Russia is the general lack of successions older than Pliensbachian. There are scattered occurrences of marine Hettangian and Sinemurian strata in northeast Russia and northern Siberia, and for the latter also in the northern Caucasus (Zakharov and Rogov 2014).

Assemblages from the lower Kovernino Formation in cores 1, 6, and 15, and from the middle and upper Kovernino Formation in core 17, differ somewhat from the previous ones. *Paleoconiferus asaccatus* is listed as present in the lower part of the formation, but the Kovernino Formation assemblages are otherwise characterized by abundant *Cerebropollenites* sp. and abundant to dominant *Classopollis* spp. (Masaitis and Pevzner 1999). Globally, *Classopollis* spp. has a long stratigraphic record with a first occurrence in the Late Triassic (see e.g., Batten and Koppelhus 1996). In Siberia, these two taxa first occur abundantly together in the early Toarcian (Goryacheva 2011; Ilyina 1985). In addition, assemblages from the middle and upper Kovernino Formation contain *Gleicheniidites* spp. and *Leptolepidites* sp., known to have their first occurrence in the early Toarcian (Goryacheva 2011).

The possibility that the Puchezh-Katunki assemblages contain palynological material reworked from older strata cannot be excluded. However, if the presence of, e.g., *P. asaccatus* in the Puchezh-Katunki assemblages is due to reworking, the question is where the reworked material came from, as pre-Bajocian Jurassic strata are missing in this area (Mitta et al. 2012). It seems more likely that a succession of Lower Jurassic strata could have been preserved within the impact crater, even if it has now been eroded in the surrounding area.

Palynological Results of Samples from the VDDH Borehole

All six samples from the VDDH borehole are primarily dominated by nonwoody plant and fungal remains. Palynomorphs generally comprise only a minor portion of the organic material. Three spore-pollen assemblages can be recognized based on the stratigraphic ranges and quantitative occurrences of the identified taxa, and these are summarized below. The full results of the palynology and, photographs of selected spores, pollen, dinoflagellate cysts, and acritarchs can be found in the supporting information.

Assemblage A occurs in the lowermost sample (V337.00) from the middle part of the unit of reworked lithic breccia and melt-bearing breccia that underlie the Kovernino Formation. It is dominated to 25% by bisaccate pollen, of which 10% are derived from corystosperms seed ferns (*Alisporites* spp.), and 6% from pinacean conifers (*Pinuspollenites minimus*). Nonsaccate conifer pollen includes thin-walled grains assigned to *Inaperturopollenites* spp. (7%), *Perinopollenites elatoides* (3%), *Auracariacites australis* (3%), *Cerebropollenites macroverrucosus* (3%), and *Classopollis torosus* (3%). Probable osmundaceous fern spores of *Cyclogranisporites* spp. (7%) and *Punctatisporites* spp. (6%) are common. The presence of *Cerebropollenites macroverrucosus* suggests an early Sinemurian maximum age (Batten and Koppelhus 1996).

Assemblage B is represented by a sample from 256.8 m in the lowermost Kovernino Formation. It is dominated by bisaccate pollen (43%), of which corystospermous seed ferns assigned to *Alisporites* spp. constitute 17% of the spore-pollen flora. Pinacean conifer pollen of *Pinuspollenites minimus* are common (9%), and cupressacean/taxodiacean conifer pollen assigned to *Perinopollenites elatoides* are abundant, making up 18% of the spore-pollen assemblage. Compared to the previous assemblage, Cheirolepidiacean conifer pollen, *Classopollis torosus* and *Classopollis meyerianus*, have increased in abundance (8%), as have *Cerebropollenites macroverrucosus* and *Cerebropollenites thiergartii* (6% and 1%, respectively). The presence of *Manumia delcourtii* and *Ischyosporites variegatus* indicates an age younger than late Pliensbachian (Batten and Koppelhus 1996). However, it should be noted that the latter taxon is also known from stratigraphic sections that encompass the Triassic–Jurassic boundary (Hillebrandt et al. 2013). Five percent of the total palynofloral assemblage consists of the fresh- to brackish-water alga *Botryococcus braunii*. but marine acritarchs, including *Leiosphaeridia* sp. and *Micrhystridium* spp., as well as dinoflagellate cysts assigned to *Mendicodinium groenlandicum* and a finely granulate form of *Mendicodinium,* are also present.

Assemblage C encompasses four samples in the lower Kovernino Formation, from 251.6 to 245.2 m. They are dominated by varying amounts of bisaccate pollen (44–66%). *Alisporites* spp. increases slightly in abundance up section from 8% to 19%. In the lowermost sample, caytonialean seed fern pollen assigned to *Vitreisporites bjuvensis* and *Vitreisporites pallidus* make up 29% of the spore-pollen flora, while in the remaining

sample these two taxa only constitute 3–5%. Cheirolepidiacean conifers, i.e., *Classopollis* spp., vary in abundance from 1 to 13%. The sample from 249.20 m contains 23% of fern spores assigned to *Deltoidospora* spp. The relative decrease in *Perinopollenites elatoides* and increase in *Spheripollenites* spp., and an abundance of *Classopollis* spp. may indicate a Toarcian age. The absence of late early to late Toarcian markers, e.g., *Callialasporites* spp., *Sestrosporites pseudoalveolatus*, and *Staplinisporites caminus*, may indicate an early Toarcian age (Batten and Koppelhus 1996; Goryacheva 2011). Marine acritarchs are most common in the lowermost sample, where *Micrhystridium* sp. and *Cymatiosphaera* sp. make up 10% of the total palynofloral assemblage, but decrease in abundance upsection. Sporadic occurrences of *Mendicodinium* sp. and putative unidentified cysts were also registered.

All three assemblages contain various amounts of reworked Triassic spores and pollen, including *Anapiculatisporites* spp., *Densoisporites playfordii*, *Lunati sporites* spp., *Lundbladispora* spp., *Protohaploxypinus samoilovichii*, and *Striatoabieites* spp. The uppermost sample also contains two specimens of *Vittatina* sp., which are assumed to be reworked from the Permian.

DISCUSSION

$^{40}Ar/^{39}Ar$ Age of the Puchezh-Katunki Impact Structure

Only one aliquot, sample 1218A, yielded a full plateau age of 193.7 ± 1.1 Ma (Fig. 7). Unfortunately, the inverse isochron intercept ratio prevents us from determining a precise $^{40}Ar/^{36}Ar$ ratio for the argon trapped in the sample, and thus to test the presence of a minor extraneous argon component. However, as (1) the data form a well-defined plateau using an $^{40}Ar/^{36}Ar$ ratio with an atmospheric composition and (2) many of the data points cluster near the radiogenic axis, thus minimizing the effect of the trapped ratio on the age measurement, we suggest that the plateau age of 193.7 ± 1.1 Ma (2σ; MSWD = 0.41; P = 0.75; including all sources of uncertainty) presented here is the best age estimate for the formation of the Puchezh-Katunki impact structure. This age is supported by the existence of one mini-plateau with an apparent age of 192.1 ± 0.6 indicating a similar age, within error, with the preferred age (193.7 ± 1.1 Ma). However, we obtained another mini-plateau age of 196.3 ± 0.8 Ma, which is not coeval with the plateau age reported above. Although somewhat supportive of the plateau age, the fact that the mini-plateau ages fully disagree further illustrates that mini-plateau apparent ages are *not suitable* to accurately date impact events (cf. Jourdan 2012; Schmieder et al. 2016). Although our plateau age is currently the most satisfying isotopic age obtained on the Puchezh-Katunki impact structure, and it is loosely supported by two mini-plateaus of relatively similar ages of 192.1 ± 0.6 and 196.3 ± 0.8 Ma, and as we will show below, by minimum palynological ages, its accuracy within the error envelope is not firmly established. Therefore, additional analyses are recommended in order to verify the age proposed in this study. For the time being, we conservatively propose that an age range of 192–196 Ma is currently the most reliable age estimate of the Puchezh-Katunki impact event and should supersede previous age recommendations. However, we currently refrain to interpret this age in the context of any biological (or the lack thereof) turnover until this age is confirmed by an additional set of concordant age data.

Ar Systematics of Unsuccessful Samples

Although one of the samples yielded a well-defined plateau age, all samples show age spectra with some level of complexity. This reflects the difficulty of dating impact melt rocks due to argon systematics originating from different phases within the impact melt rocks.

In the present case, most of the spectra shapes can be explained by a combination of inherited $^{40}Ar^*$, either resulting from clasts observed in thin sections (e.g., sample V931) or simply trapped in the melt rock during the melting stage, both resulting in apparent step ages that are older than the impact age. Conversely, another effect that seems to plague some of the samples is the presence of alteration products, due to impact-induced hydrothermal circulation in, or later alteration of, the samples and resulting in apparent step ages that are younger than the impact age (e.g., Jourdan et al. 2010; Schmieder et al. 2014, fig. 5). Regardless, from our study, it is clear that there is not necessarily a simple relationship between petrographic findings on an impact melt rock sample and behavior of an $^{40}Ar/^{39}Ar$ age spectrum, in particular when cryptic inherited $^{40}Ar^*$ is present in the melt (Jourdan et al. 2007). This effect is demonstrated in our study by variable resultant age spectra, even when duplicate samples are analyzed. This is likely due to the mixture of components and phases in the impact melt samples and the possible heterogeneous shock metamorphism and melting commonly observed within the same sample.

Implications from Palynology of the Crater Sediments

Both the results of the new palynological analysis of the VDDH samples, as well as the re-evaluation of the palynological assemblages previously reported as Bajocian to Bathonian by Masaitis and Pevzner (1999), indicate a much older depositional age for the crater

sediments, namely Sinemurian–Pliensbachian to early Toarcian. This is somewhat surprising, considering that Early Jurassic sediments are otherwise lacking in the area. In addition, the presence of marine acritarchs and rare dinoflagellate cysts in the samples from the lower Kovernino Formation was unexpected, as the crater infill has previously been described as fully lacustrine (Masaitis and Pevzner 1999). However, from a structural point of view, it is not unlikely that a succession of Early Jurassic sedimentary rocks could be preserved within the crater, even if they have been removed from the surrounding area. In an interpretation of the structural geology of the impact area, Kolodyazhnyi (2014) interpreted the so-called "Coptomict Gravelite" (redeposited lithic breccia and melt-bearing breccia underlying the Kovernino Formation) as being Early Jurassic in age, and the Kovernino Formation as Bajocian–Bathonian following Masaitis and Pevzner (1999). The palynological assemblage from the unit of redeposited breccia analyzed herein suggests that deposition took place in a freshwater environment during the Sinemurian–Pliensbachian, although a single specimen of *Leiosphaeridia* sp. was recorded, which may indicate some minor marine influence. There are no palynological indications that the unit of redeposited breccia was deposited during the Middle Jurassic. The palynological assemblages from the lower Kovernino Formation indicate a depositional age younger than the late Pliensbachian, based on the first occurrences of *Manumia delcourtii*, *Ischyosporites variegatus*, and the marine dinoflagellate cyst *Mendicodinium groenlandicum* (Appendices S3–S5 in supporting information). A marginal marine, probably lagoonal setting is suggested, not only by the presence of *Mendicodinium* spp., but also by the occurrence of marine acritarchs *Micrhystridium stellatum*, *Micrhystridium intromittum* and *Leiosphaeridia* sp. (see Appendices S3 and S5). The lack of Early Jurassic strata on the Russian Platform necessitates correlation with other areas. Marine sediments of Pliensbachian–Toarcian age are known from the surrounding region in the northern Caucasus area (Jaroshenko 1965), western and northern Siberia (Zakharov et al. 2006; Zakharov and Rogov 2014), and also from the Polish Basin (Hesselbo and Pienkowski 2011) and northwestern Europe (see e.g., Ruhl et al. [2016] and references therein). There is currently no stratigraphic evidence that the lower Kovernino Formation was deposited during the Middle Jurassic. Typical Middle Jurassic taxa, such as *Callialasporites* spp., *Sestrosporites pseudoalveolatus*, *Staplinisporites caminus*, *Leptolepidites* spp., and *Gleicheniidites senonicus* that are usually common in Middle Jurassic palynofloras (Batten and Koppelhus 1996) are completely lacking in the lower Kovernino Formation. Thus, we favor the interpretation that the crater sediments, including the redeposited breccia unit and the overlying lower Kovernino Formation, were deposited during the late Early Jurassic, most probably during the Pliensbachian (~191–183 Ma) to early Toarcian (~183–174 Ma; Cohen et al. 2013).

CONCLUSIONS

A new, narrowed age range of 192–196 Ma is presented for the formation of the Puchezh-Katunki impact structure, located ~400 km northeast of Moscow (Russia). We propose that the impact structure was formed during this age range based on $^{40}Ar/^{39}Ar$ analyses and the statistical relevance of the obtained age plateau and mini-plateaus, linked with our petrographic observations of the investigated samples. Our results show that there is not necessarily a simple relationship between the observed petrographic features of an impact melt rock sample and the obtained $^{40}Ar/^{39}Ar$ age spectra and inverse isochrons. The new age estimate obtained with the $^{40}Ar/^{39}Ar$ method is fully supported by our newly revised biostratigraphy of sediments and breccias from the Puchezh-Katunki impact structure, which all imply a late Sinemurian to early Pliensbachian age for the impact event.

Acknowledgments—We thank Martin Schmieder and Uwe Reimold for their thorough and constructive reviews that improved the manuscript. We also want to thank Michael Poelchau for editorial comments that improved the manuscript. Jo-Anne Wartho and Igor Villa are thanked for helpful comments and suggestions on a previous version of this manuscript. The authors greatly appreciate the help from Prof. Em. Svetlana Bogdanova with the Russian literature and for the handling of the investigated samples. P. Carlgren is thanked for assisting with translations of Russian references. This study was funded by grants from the Swedish Research Council (grant no. 2017-06388) to S.H.-A. and (grant no. 621-2012-4504) to C.A. and from the Crafoord Foundation (grant no. 20140617) to C.A. M.M. was supported by a Swiss National Science Foundation Ambizione grant.

Editorial Handling—Dr. Michael Poelchau

REFERENCES

Batten D. J. and Koppelhus E. B. 1996. Biostratigraphic significance of uppermost Triassic and Jurassic miospores in Northwest Europe. In *Palynology: Principles and applications*, edited by Jansonius J. and McGregor D. C. Dallas, Texas: American Association of Stratigraphical Palynologists Foundation, vol. 2. pp. 795–806.

Bogorodskaya O. A. and Tumanov R. R. 1980. Geological map of USSR of 1:200 000 scale. Sheet O-38-XXVI, Explanatory notes. Moscow: Nedra Press. 130 p.

Bolkhovitina N. A. 1956. Atlas of spores and pollen from Jurassic and Lower Cretaceous deposits of the Vilyui depression. *Transactions of the Institute of Geology, Academy of Sciences, USSR* 2:1–188. In Russian.

Bolkhovitina N. A. 1959. Spore-pollen complexes of the Mesozoic deposits of the Vilyuysk depression and their stratigraphic significance. *Proceedings of the Geological Institute of the Russian Academy of Sciences* 24:1–185. In Russian.

Bottomley R. J., York D., and Grieve R. A. F. 1990. ^{40}Argon-^{39}argon dating of impact craters (abstract). 20th Lunar and Planetary Science Conference. pp. 421–431.

Cohen K. M., Finney S. C., Gibbard P. L., and Fan J.-X. 2013; updated. The ICS International chronostratigraphic chart. *Episodes* 36:199–204.

Dobrutskaja N. A. 1968. Spore-pollen assemblages from the Middle and Upper Jurassic deposits of the northern part of Russian Platform. Palaeopalynological method in stratigraphy. Materials for 2nd International Palynological Conference Holland, September 1966, Leningrad, pp. 71–81.

Earth Impact Database. http://www.passc.net/EarthImpactDatabase/. Accessed November 18, 2019.

Feld'man V. I., Sazonova L. V., and Nosova A. A. 1984. The geological structure and petrography of impactites of the Puchezh-Katunki astrobleme (Volga Region). *Byulleten' Moskovoskogo Obshchestva Ispytatelei Prirody, Otd. Geol.* 59:53–63. In Russian.

Ferrière L., Koeberl C., and Reimold W. U. 2009. Characterization of ballen quartz and cristobalite in impact breccias: New observations and constraints on ballen formation. *European Journal of Mineralogy* 21:203–217. https://doi.org/10.1127/0935-1221/2009/0021-1898.

Firsov L. 1973. Concerning the meteoritic origin of the Puchezh-Katunki crater. *Meteoritics* 8:223–244. https://doi.org/10.1111/j.1945-5100.1973.tb01251.x.

Goryacheva A. A. 2011. Palynostratigraphy of the Lower-Middle Jurassic deposits, borehole section Vostok 4 (Southeast of West Siberia). *Stratigraphy and Geological Correlation* 19:268–288. https://doi.org/10.1134/S086959381103004X.

Grieve R. A. F., Osinski G. R., and Chanou A. 2015. The suevite conundrum: A general perspective (abstract). Bridging the Gap III, Freiburg. p. 1036.

Hesselbo S. P. and Pienkowski G. 2011. Stepwise atmospheric carbon-isotope excursion during the Toarcian oceanic anoxic event (Early Jurassic, Polish Basin). *Earth and Planetary Science Letters* 301:365–372. https://doi.org/10.1016/j.epsl.2010.11.021.

Hillebrandt A. V., Krystyn L., Kürschner W. M., Bonis N. R., Ruhl M., Richoz S., Schobben M. A. N., Urlichs M., Bown P. R., Kment K., McRoberts C. A., Simms M., and Tomãsových A. 2013. The global stratotype sections and point (GSSP) for the base of the Jurassic system at Kuhjoch (Karwendel Mountains, Northern Calcareous Alps, Tyrol, Austria). *Episodes* 36:162–198.

Ilyina V. I. 1985. *Palynology of the Jurassic in Siberia*. Moscow, Russia: Nauka. pp. 3–237 [In Russian].

Ilyina V. I. 1986. Subdivision and correlation of the marine and non-marine Jurassic sediments in Siberia based on palynological evidence. *Review of Palaeobotany and Palynology* 48:357–364. https://doi.org/10.1016/0034-6667(86)90073-4.

Jaroshenko O. P. 1965. Spores and pollen complexes of Jurassic and Lower Cretaceous deposits of northern Caucasus and their stratigraphic importance. *Transactions of the Academy of Science–USSR* 117:1–134.

Jourdan F. 2012. The ^{40}Ar/^{39}Ar dating technique applied to planetary sciences and terrestrial impacts. *Australian Journal of Earth Sciences* 59:199–224. https://doi.org/10.1080/08120099.2012.644404.

Jourdan F., Renne P. R., and Reimold W. U. 2007. The problem of inherited ^{40}Ar* in dating impact glass by ^{40}Ar/^{39}Ar geochronology: Evidence from the Tswaing crater (South Africa). *Geochimica et Cosmochimica Acta* 71:1214–1231. https://doi.org/10.1016/j.gca.2006.11.013.

Jourdan F., Schmieder M., and Buchner E. 2010. The Lake Saint Martin impact and the problem of isotopic dating on altered impact melt rocks (abstract #1654). 41st Lunar and Planetary Science Conference. CD-ROM.

Jourdan F., Reimold W. U., and Deutsch A. 2012. Dating terrestrial impact structures. *Elements* 8:49–53. https://doi.org/10.2113/gselements.8.1.49.

Kelley S. 2002. Excess argon in K-Ar and Ar–Ar geochronology. *Chemical Geology* 188:1–22. https://doi.org/10.1016/S0009-2541(02)00064-5.

Kolodyazhnyi S. Y. 2014. Structural assemblies of the Vladimir-Vyatka dislocation zone and the position of the Puchezh-Katunki Crater, East European Platform. *Geotectonics* 48:104–121. https://doi.org/10.1134/S0016852114020046.

Masaitis V. L. 1999. Impact structures of northeastern Eurasia: The territories of Russia and adjacent countries. *Meteoritics & Planetary Science* 34:691–711. https://doi.org/10.1111/j.1945-5100.1999.tb01381.x.

Masaitis V. L., and Pevzner L. A. 1999. *Deep drilling in the Puchezh-Katunki impact structure*. Saint Petersburg, Russia: VSEGEI-Press. 350 p. In Russian.

Masaitis V. L., Mashchak M. S., and Naumov M. V. 1996. The Puchezh-Katunki astrobleme: A structural model of a giant impact crater. *Solar System Research* 30:3–10.

Mashchak M. S. 1999. Dating of the impact event. In *Deep drilling in the Puchezh-Katunki impact structure*, edited by Masaitis V. L. and Pevzner L. A. Saint Petersburg, Russia: VSEGEI-Press. pp. 242–244. In Russian.

McDougall I., and Harrison T. M. 1999. *Geochronology and thermochronology by the ^{40}Ar/^{39}Ar method*. Oxford, UK: Oxford University Press. 288 pp.

Mitta V. V., Vuks V. J., Glinskikh L. A., Dzyuba O. S., Zakharov V. A., Kirikov V. P., Kostyleva V. V., Maleonkina S. J., Nikitenko B. L., Pestchevitskaya E. B., Rogov M. A., Rostovtseva J. I., Seltser V. B., and Tesakova E. M. 2012. Unified regional stratigraphic scheme of the Jurassic of East European Platform, explanatory note. In *Paleontological Institute of RAS (PIN) & All-Russian Geological Oil Institute (VNIGNI)*, edited by Mitta V. V., Alekseev A. S., and Shik S. M. Moscow, Russia 63 p.

Nielsen L. H., Petersen H. I., Dybkjær K., and Surlyk F. 2010. Lake-mire deposition, earthquakes and wildfires along a basin margin fault; Rønne Graben, Middle Jurassic, Denmark. *Palaeo3* 292:103–126. https://doi.org/10.1016/j.palaeo.2010.03.032.

Pálfy J. 2004. Did the Puchezh-Katunki impact trigger an extinction? In *Cratering in marine environments and on ice*,

edited by Dypvik H., Burchell M. and Claeys P. Berlin, Germany: Springer Verlag. pp. 135–148.

Renne P. R., Swisher C. C., Deino A. L., Karner D. B., Owena T. L., and DePaolo D. J. 1998. Intercalibration of standards, absolute ages and uncertainties in $^{40}Ar/^{39}Ar$ dating. *Chemical Geology* 145:117–152. https://doi.org/10.1016/S0009-2541(97)00159-9.

Renne P., Balco G., Ludwig K. R., Mundil R., and Min K. 2011. Response to the comment by W.H. Schwarz et al. on "Joint determination of ^{40}K decay constants and $^{40}Ar*/^{40}K$ for the Fish Canyon sanidine standard, and improved accuracy for $^{40}Ar/^{39}Ar$ geochronology" by P.R. Renne et al. (2010). *Geochimica et Cosmochimica Acta* 75:5097–5100. https://doi.org/10.1016/j.gca.2011.06.021.

Rostovtseva J. I. 2013. Palynological characteristics of Kudinovo Formation (Middle Jurassic) in Moscow region. *Bulletin of Moscow Society of Naturalists* 88:15–21.

Rostovtseva J. I. 2014. The palynological assemblages of the Middle Jurassic of the Russian Platform (abstract). 9th European Palaeobotanical and Palynological Conference, Padova. pp. 235–236.

Ruhl M., Hesselbo S. P., Hinnov L., Jenkyns H. C., Xu W., Riding J. B., Storm M., Minisini D., Ullmann C. V., and Leng M. J. 2016. Astronomical constraints on the duration of the early Jurassic Pliensbachian Stage and global climatic fluctuations. *Earth and Planetary Science Letters* 455:149–165. https://doi.org/10.1016/j.epsl.2016.08.038.

Schmieder M. and Buchner E. 2008. Dating impact craters: palaeogeographic versus isotopic and stratigraphic methods–A brief case study. *Geological Magazine* 145:586–590. https://doi.org/10.1017/S0016756808005049.

Schmieder M., Schwarz W. H., Buchner E., Trieloff M., Moilanen J., and Öhman T. 2010. A Middle-Late Triassic 40Ar/39Ar age for the Paasselkä impact structure (SE Finland). *Meteoritics & Planetary Science* 45:572–582. https://doi.org/10.1111/j.1945-5100.2010.01041.x.

Schmieder M., Jourdan F., Tohver E., and Cloutis E. A. 2014. $^{40}Ar/^{39}Ar$ age of the Lake Saint Martin impact structure (Canada)ucode > –Unchaining the Late Triassic terrestrial impact craters. *Earth and Planetary Science Letters* 406:37–48. https://doi.org/10.1016/j.epsl.2014.08.037.

Schmieder M., Schwarz W. H., Trieloff M., Tohver E., Buchner E., Hopp J., and Osinski G. 2015. New $^{40}Ar/^{39}Ar$ dating of the Clearwater Lake impact structures (Québec, Canada)–Not the binary asteroid impact it seems? *Geochimica et Cosmochimica Acta* 148:304–324. https://doi.org/10.1016/j.gca.2014.09.037.

Schmieder M., Schwartz W. H., Buchner E., Trieloff M., Hopp J., Tohver E., Pesonen L. J., Lehtinen M., Moilanen J., Werner S. C., and Öhman T. 2016. The two Suvasvesi impact structures, Finland: Argon isotopic evidence for a "false" impact crater doublet. *Meteoritics & Planetary Science* 51:966–980. https://doi.org/10.1111/maps.12636.

Steiger R. and Jäger E. 1977. Subcommission on geochronology: Convention on the use of decay constants in geo- and cosmochronology. *Earth and Planetary Science Letters* 36:359–362. https://doi.org/10.1016/0012-821X(77)90060-7.

Stöffler D. 2015. The suevite conundrum: New concepts for the Ries crater–A retake (abstract). Bridging the Gap III. Freiburg, Germany. p. 1002.

Zakharov V. and Rogov M. 2014. Review of the Jurassic system of Russia: Stages, boundaries, and perspectives. In *STRATI 2013*, edited by Rocha R., Pais J., Kullberg J., and Finney S. Basel, Switzerland: Springer International Publishing. pp. 629–634.

Zakharov V. A., Shurygin B. N., Il'ina V. I., and Nikitenko B. L. 2006. Pliensbachian–Toarcian biotic turnover in North Siberia and the Arctic region. *Stratigraphy and Geological Correlation* 14:399–417. https://doi.org/10.1134/s0869593806040046.

SUPPORTING INFORMATION

Additional supporting information may be found in the online version of this article:

Appendix S1. Full isotopic argon data, with ratios, percentage of gas release, and age data for all the individual sample steps of each of the samples.

Appendix S2. Full results of the new palynological age estimates of samples from the Puchezh-Katunki impact structure.

Appendix S3. Range chart showing the palynology and chronostratigraphy of the Gritstone and standstone unit and the lower Kovernino Formation in VDDH.

Appendix S4. Plate I. Selected spores and pollen from the Vorotilovskaya deep drill hole, with sample, slide number, and England Finder coordinates.

Appendix S5. Plate II. Selected pollen, dinoflagellate cysts and acritarchs from the Vorotilovskaya deep drill hole, with sample, slide number, and England Finder coordinates.